Polarized photoluminescence from point emitters in ordered $Ga_xIn_{1-x}P$

B. Fluegel, A. Mascarenhas, and J. F. Geisz
National Renewable Energy Laboratory, 1617 Cole Boulevard, Golden, Colorado 80401, USA
(Received 5 May 2009; revised manuscript received 27 July 2009; published 29 September 2009)

A wide-field microphotoluminescence study of ordered $Ga_xIn_{1-x}P$ reveals spatially isolated submicron emission centers that emit in a spectral band 20 meV below previously studied PL features. The density of these centers is correlated with the presence of sharp PL lines reported in the low-energy PL band. Polarization analysis shows that many centers are very highly linearly polarized, contrary to models of quantum disks aligned at antiphase boundaries normal to the ordering direction. Orientations of the linearly polarized centers are found in some cases to be highly aligned along specific crystal directions that are not simply related to ordering.

DOI: 10.1103/PhysRevB.80.125333 PACS number(s): 78.66.Fd, 78.55.Cr, 71.20.Nr, 71.55.Eq

I. INTRODUCTION

The intrinsic structural and band structure changes caused by spontaneous ordering that occur in MOVPE-grown $Ga_xIn_{1-x}P$ are well understood (see Ref. 1 for a review). Under specific growth conditions (temperature, III-V ratio and substrate orientation) the Ga and In atoms distribute not as a random alloy, but with long-range ordering into a superlattice of alternating indium-rich and gallium-rich monolayers along the $[111]_B$ ordering direction. The degree to which ordering occurs is expressed as an ordering parameter, η, defined such that the alternating monolayers have compositions $Ga_{x+\eta/2}In_{1-x-\eta/2}P$ and $Ga_{x-\eta/2}In_{1-x+\eta/2}P$. An alloy of $x=0.52$ is lattice matched to the GaAs substrate and ordering parameters as high as 0.55 with domains that extend laterally up to 0.5 μm have been attained. This results in band-gap lowering and valence band splitting in this technologically important material. In addition to these effects, spontaneous ordering is accompanied by defect-induced changes in the photoluminescence (PL) spectrum which are still poorly understood. Several tens of meV below the bandgap, a broad low-energy band (LEB) is uniformly present, and on a microscopic scale, extremely sharp low-energy spectral lines (LEL) are seen throughout the same spectral region in some samples.[2,3] Even under submicron spatial resolution, multiple sharp (100 μeV) lines are found whose energies vary rapidly with sample position. To explain these sharp discrete energies, a type of quantum disk was proposed[4] based on an antiphase boundary (APB), i.e., a stacking fault that creates a double layer of indium-rich material within the partially ordered GaInP host material. Strong experimental evidence was presented[4] including an anisotropic diamagnetic shift that peaked for $\boldsymbol{B}$ oriented along the ordering axis, and a correlation between LEL density and APB density. A detailed calculation[5] found that the band alignment between the double In layer and the GaInP host would be type II, and this was thought to explain the extremely long PL lifetimes found[6,7] in the LEB.

However, later studies did not support that particular quantum disk as an origin of the LEL or LEB, as the correlation between LEL and APB density was not confirmed[8] and the magnetic field orientation dependence of the diamagnetic shift was found to be smaller than the random distribution among LEL.[9] Measurements showed that the very long lifetimes of the LEB PL did not extend also to the LEL,[8,10] and thus, a model of a type-II quantum disk was not supported. Furthermore, it was argued[8] that the APBs, which are spatially quite dilute in large-domain samples, could not be the source of spectral components that exist throughout the entire sample. The detailed spatial maps that have been made[8] of the LEB exhibit relatively low contrast, i.e., that signal is everywhere nonzero. Similarly, the LEL are sparse only for a particularly energy, but if the full spectrum of possible LEL energies is considered, that integrated signal can be found throughout certain samples, even when the experimental spatial resolution is capable of isolating single domains. It has been proposed that the LEL arise not from the long extended APBs seen in transmission electron microscopy (TEM), but rather from finer boundaries of domains that are only 5–10 nm in size.[11] An origin on this scale is unexpected since the LEL first begin to be resolved when the experimental spatial resolution is decreased to a few microns, a threshold that is much closer to the size of the larger domains.

The present study takes a wide-field approach to studying this spatial dependence. Where previous studies used point-by-point raster scans to build up a PL map, or ensembles of fixed apertures to acquire statistics, these techniques were limited in the amount of sample that could be studied. For example, samples that were previously claimed to be absent of LEL can now be observed to exhibit them at a very low density. The ability to study single *isolated* defects is greatly enhanced when large regions of sample can be surveyed. Here, we study the polarization properties of individual defects and the statistics of those defects throughout the sample.

II. EXPERIMENT

The PL mapping used here is a direct-imaging technique in which the entire two-dimensional (2D) sample surface is imaged onto an electron-multiplying charge-coupled device camera with a magnification of 50×. Spectral resolution is obtained using a liquid crystal tunable filter (LCTF) that dynamically selects the PL band of interest. Samples are held in a microcryostat and illuminated axially with a white light, or obliquely with a 532 nm laser. The white light or PL is col-

TABLE I. Growth conditions, peak energy of low-temperature heavy hole to conduction band photoluminescence, order parameter, and original reference for the ordered GaInP samples. $E_{HH\text{-}CB}$ was updated for the wafer segments used in the present study. The order parameter was calculated as in Ref. 12 without correction for composition variation.

Sample	Described in Ref.	Growth temperature	Growth Rate (μm/hr)	Substrate	V/III ratio	$E_{HH\text{-}CB}$ (eV)	Order parameter
A	16	680 °C	3	6° $[111]_B$	100	1.907	0.46
B	3 (sample 2)	680 °C	4	6° $[111]_B$	70	1.901	0.47
C	3 (sample 1)	690 °C	4	4° $[111]_B$	70	1.917	0.43

lected with a 0.65 numerical aperture objective that is compensated for the spherical aberration of the cryostat window. The light is then passed through the LCTF and focused onto the camera chip, or alternatively, unfiltered discrete image points may be projected onto the tip of a single-mode fiber that is coupled to a spectrometer. Images and spectra both have a spatial resolution of approximately 1 μm. The absorbed laser power density is 0.5 W/cm^2, which is well below the density at which the LEL have been observed to saturate.[3,4,10] The bandpass is selectable between 0.5 or 5 nm and all data were taken at 7 K.

The data presented here are from samples A–C, previously characterized in the references shown in Table I. All have large order parameters and are grown on GaAs substrates miscut 4° or 6° toward $[111]_B$ and with thicknesses of 10 microns, resulting in large single-variant domains. With regard to the occasionally conflicting past results described above for the below band-gap states, we have also examined a series of MOVPE samples grown at a second growth facility.[12] Growth conditions were similar to samples A–C resulting in comparable values for band-gap reduction, linewidths, and valence-band splitting.

III. RESULTS

The wide-field PL images that we obtain agree well with published[8] maps of the excitonic, or high-energy PL (HE) and the LEB. For those spectral regions, PL is roughly homogeneous, with a fine structure that is likely domain boundaries. By further tuning the bandpass filter to an energy just below the LEB/LEL, rare features of low-emission energy show up as a dark field image. Comparison with visible optical microscopy confirms that the low-energy features presented here occur in regions of otherwise pristine sample that are free from any fractures, pits or gross surface contaminants. Figures 1(a) and 1(b) show PL maps for samples A and B, whose LEL were studied in Ref. 8. Both samples have large domain size and strong ordering, yet exhibited very different densities of LEL: sample B has one of the most densely structured LEL, whereas no LEL could be found in sample A.[8] Figure 1 shows that there is also a similar presence and absence of spatially discrete PL emitters that we now term point emitters (PE). These point-like spots are smaller than the optical system resolution and by selecting a single PE with the fiber/spectrometer, it can be seen that they are distinguished by an emission band approximately

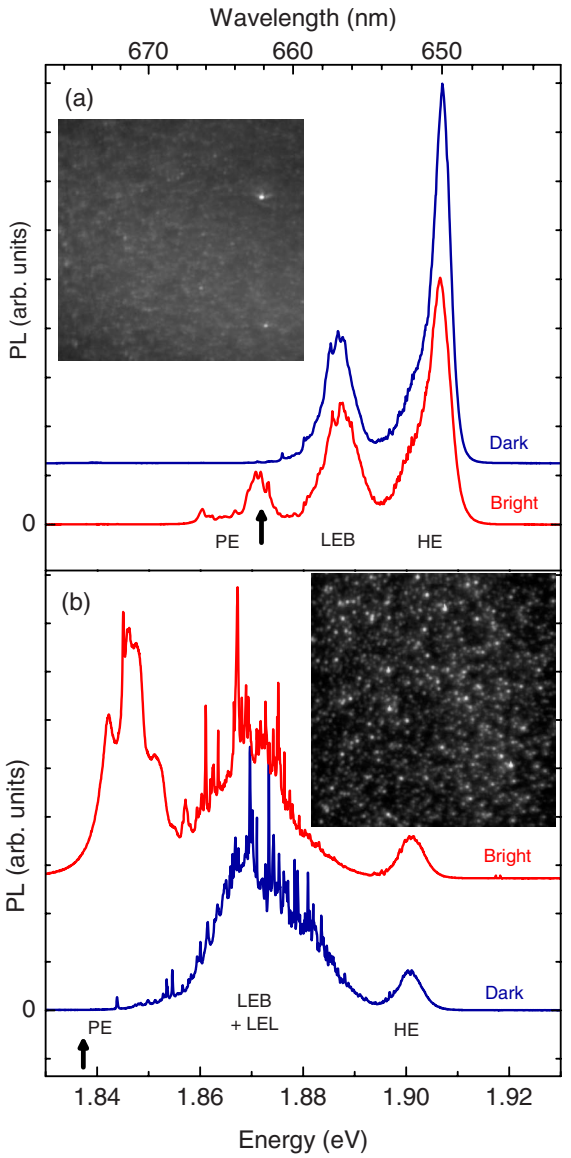

FIG. 1. (Color online) PL maps and single-point spectra of two GaInP samples that have (a) very few and (b) very dense LEL. Spectra are displaced vertically for clarity and curves labeled "bright" and "dark" are taken at a single PE and at a region removed from the PE, respectively. Labels identify the different spectral regions where important features occur in ordered GaInP and vertical arrows identify the filter wavelength used for the image. Maps are 80×80 μm^2.

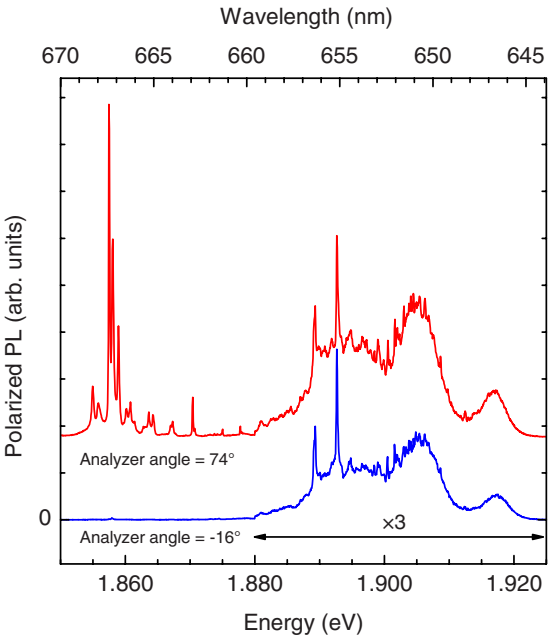

FIG. 2. (Color online) Polarized PL spectra of a PE point, displaced vertically for clarity. Both curves are expanded in the high-energy region shown by the horizontal arrow. Analyzer angles are relative to the surface projection of the ordering axis.

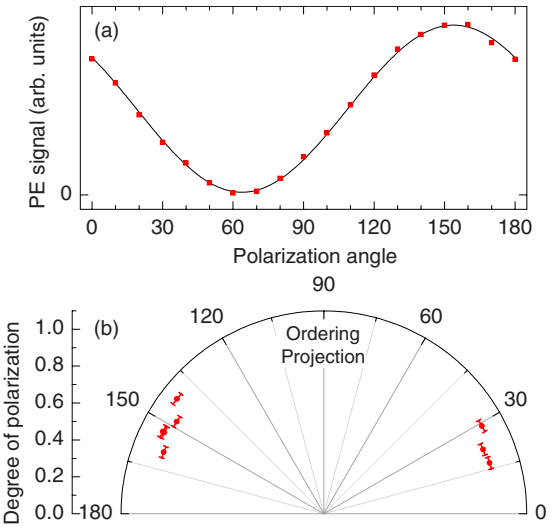

FIG. 3. (Color online) Polarization of PL emitted by low-energy points in sample C. (a) Level of signal at 661.2 nm from one point emitter as a function of analyzer angle. Solid line is a fit of the data points to a sinusoid+constant. (b) Angle of maximum signal and degree of polarization extracted as in (a), plotted for several PE. Error bars are due to finite bandwidth and extinction ratio of the LCTF. Angles are relative to [110], i.e., offset 90° from Fig. 2.

20 meV below the LEB. The specific spectral shape of the PE varies considerable from point to point and may contain both broadened features as in Fig. 1 or lines as sharp as 100 μeV. Thus, they are spectrally similar to the LEB +LEL region, yet distinguished by their microscopic spatial extent.

We now examine the degree of linear polarization, P, of this PL band, where $P \equiv \frac{I_{\parallel}-I_{\perp}}{I_{\parallel}+I_{\perp}}$ with $I_{\parallel}$ and $I_{\perp}$ the PL signals parallel to and orthogonal to a reference axis. Figure 2 shows polarized PL of sample C showing all the GaInP spectral components. The PE region (1.85–1.88 eV) exhibits more resolved lines and fewer broadened components compared to the samples in Fig. 1. The moderate degree of polarization seen in the HE and LEB measured in low-temperature PL has been thoroughly studied[12–14] and can be understood by considering the effect of ordering to be perturbatively described as a crystal-field splitting. Since the resulting $[1\bar{1}1]$ uniaxis is skewed to the (001) surface, the polarization measured at this surface is partial: the $[1\bar{1}0]$ direction is the surface projection of the ordering axis, along which PL from HH-CB recombination is forbidden. In contrast, the [110] polarization direction is orthogonal to that axis and hence PL is fully allowed. The observed degree of polarization of the HE PL in the epilayer plane is reduced from a theoretical value of 0.5 to the typical range 0.3–0.4 due to effects of substrate misorientation and excitonic binding.[14] In the case of the sharp spectral lines, however, the polarization has not been previous reported. If we concentrate on sharp lines that are strong and well-resolved from the LEB background such as near 1.89 eV, then the two orthogonally polarized spectra in Fig. 2 reveal that the LEL does not have the same orientation and degree of polarization that is shared by the broad spectral components. More detailed measurements show that the LEL is less polarized. It is therefore surprising to see that in the PE region the sharp lines are very highly polarized, with a degree of polarization $P > 0.99$ for the strong spectral line near 1.857 eV. The degree of polarization and consistency among different PE varied between samples, but in all samples that showed the PE, instances were found of polarization higher than expected from the crystal field splitting.

The orientation of the PE polarization is also unexpected. The polarizations of the two spectra in Fig. 2 are oriented parallel and orthogonal to an axis that is not along the surface projection of the ordering axis, but approximately 16° off from it. The deviation was found to be very consistent in this sample. By acquiring polarized images filtered at a narrow-band energy within the PE spectral region, the statistical distribution of polarization can be studied for all points emitting at that energy. Figure 3(a) shows this signal spatially integrated over a single PE and plotted as a function of polarization angle. A sinusoidal fit is used to extract values for the orientation and degree of polarization. These values, for a set of randomly selected PE are shown in Fig. 3(b). In each case, the polarization was near unity, and the orientations were strongly clustered in two directions that are symmetrically spaced on either side of the ordering projection. While not all PE in the field (>100) were digitized for this figure, a visual inspection of the central 90° polarization image confirmed the conclusion of Fig. 3(b): none of the PE reached a maximum near that angle.

IV. DISCUSSION

The connection suggested by Fig. 1 between the density of PE seen in the PL image, and the density of sharp lines

seen in the PL spectrum was repeated in many samples. For reasons not known, samples with strong LEL are a minor subset of ordered GaInP samples, as are samples showing PE, yet these two subsets are nearly identical with a direct dependence between densities of LEL and PE. This was also found in a set of eight high-quality ordered samples grown in the second growth facility. A possible explanation for the correlation between the two features may be that the PE arise from pairing of the unknown defects that cause the LEL. When that defect density is high, there exists a strong probability for the measurement to observe pairs of defects close enough to form a joined potential well. PL from recombination of carriers bound to this well would have a lower emission energy and a distinct polarization direction due in part to the symmetry of the pair. Known examples of close pairs, separated by a single lattice constant, occur with impurities in the isoelectronically doped semiconductor GaAs:N.[15] In this case the pairing results in a state with much lower density than the parent impurity and PL with a lower photon energy and a linear polarization dictated by the orientation of the pair. This is all consistent with the present PE data.

The specific polarization directions shown in Fig. 3(b) are more difficult to explain. It would appear, however, that the host's symmetry of C_{3V} along $[1\bar{1}1]$ is not maintained at the PE location, since the PE PL is so strongly polarized in the plane of the sample's surface. The polarization would instead suggest a geometry that is linear and parallel to the surface, or planar aligned normal to the surface. This is not ruled out by the unchanged HE spectrum found at the PE locations (bright spectra in Fig. 1). That HE peak confirms that PE are situated in regions of uniform host sample, but it need not be indicative of the defect volume itself, since the local disruptions to the ordering symmetry could be small (20 lattice spacings was used for calculations in Ref. 5) compared to the one-micron sampling volume. In addition, the polarization of the LEL in Fig. 2 are problematic as well, since that weak polarization contradicts the result expected for heavy hole to conduction band recombination in $[1\bar{1}1]$ ordered GaInP, and it also contradicts the very similar symmetry expected from the quantum disks of Ref. 5. However, as we have noted, a type-II quantum disk formed at that type of APB is more specific than the experimental evidence supporting it. As pointed out in Ref. 8, APBs need not be along the ordering planes. In fact TEM images do not show such a simple picture.[8,11,16] In Ref. 11, cross-sectional scanning tunneling microscopy was used to show that TEMs may give an incomplete picture, and that APBs which appear to poorly follow a particular lattice plane can actually be analyzed into multiple small segments each well aligned with one of a small number of lattice planes. The relative contribution and orientation of the two dominant planes agreed with the intensity and polarization of two broad, below gap, spectral peaks in the cathodoluminescence detected near such an APB.[11] Without greater information on their spatial dependence, it is difficult to identify them with the spectrally sharp, spatially dilute features in Figs. 1 and 2, however it is clear that quantum disks can be oriented in directions other than the ordering axis.

Previous studies of the LEL have struggled with the large distribution of the sharp line energies. Even when the probing diameter is reduced to as small as 200 nm and many such volumes are examined, no general quantitative pattern in energies or energy spacings emerges. This apparent randomness forces the assumption of strong disorder in the size and shape of the proposed confining potential. The same holds true for the sharp lines in the PE. However, the experimental polarization behavior presented in this study is a rare instance of a common behavior for these defects that is not dominated by the disorder. It applies to all lines within the PE region and to many PE across the sample. This general behavior suggests that a well-defined origin may be found for the PE and by association with it, the LEL.

ACKNOWLEDGMENTS

We acknowledge the financial support of the Department of Energy Office of Science, Basic Energy Sciences under Grant No. DE-AC36-08GO28308. We thank Yong Zhang and S. P. Ahrenkiel for critical discussions and P. Ernst for use of samples.

[1] *Spontaneous Ordering in Semiconductor Alloys*, edited by A. Mascarenhas, D. Follstaedt, T. Suzuki, and B. Joyce (Materials Research Society, Pittsburgh, 1999).
[2] U. Kops, R. G. Ulbrich, M. Burkard, C. Geng, F. Scholz, and M. Schweizer, Phys. Status Solidi A **164**, 459 (1997).
[3] H. M. Cheong, A. Mascarenhas, J. F. Geisz, J. M. Olson, M. W. Keller, and J. R. Wendt, Phys. Rev. B **57**, R9400 (1998).
[4] U. Kops, P. G. Blome, M. Wenderoth, R. G. Ulbrich, C. Geng, and F. Scholz, Phys. Rev. B **61**, 1992 (2000).
[5] T. Mattila, Su-Huai Wei, and Alex Zunger, Phys. Rev. Lett. **83**, 2010 (1999).
[6] M. C. DeLong, W. D. Ohlsen, I. Viohl, P. C. Taylor, and J. M. Olson, J. Appl. Phys. **70**, 2780 (1991).
[7] P. Ernst, C. Geng, F. Scholz, and H. Schweizer, Phys. Status Solidi B **193**, 213 (1996).
[8] S. Smith, A. Mascarenhas, S. P. Ahrenkiel, M. C. Hanna, and J. M. Olson, Phys. Rev. B **68**, 035310 (2003).
[9] S. Smith, A. Mascarenhas, and J. M. Olson, Phys. Rev. B **68**, 153202 (2003).
[10] B. Fluegel, S. Smith, Y. Zhang, A. Mascarenhas, J. F. Geisz, and J. M. Olson, Phys. Rev. B **65**, 115320 (2002).
[11] Y. Ohno, Phys. Rev. B **72**, 121307(R) (2005).
[12] P. Ernst, C. Geng, F. Scholz, H. Schweizer, Y. Zhang, and A. Mascarenhas, Appl. Phys. Lett. **67**, 2347 (1995).
[13] G. S. Horner, A. Mascarenhas, R. G. Alonso, S. Froyen, K. A. Bertness, and J. M. Olson, Phys. Rev. B **49**, 1727 (1994).
[14] Y. Zhang, A. Mascarenhas, P. Ernst, F. A. J. M. Driessen, D. J. Friedman, K. A. Bertness, and J. M. Olson, J. Appl. Phys. **81**, 6365 (1997).
[15] S. Francoeur, J. F. Klem, and A. Mascarenhas, Phys. Rev. Lett. **93**, 067403 (2004).
[16] H. M. Cheong, A. Mascarenhas, S. P. Ahrenkiel, K. M. Jones, J. F. Geisz, and J. M. Olson, J. Appl. Phys. **83**, 5418 (1998).